Proceedings of the 9th International Conference of Control Systems, and Robotics (CDSR'22)
Niagara Falls, Canada – June 02-04, 2022
Paper No. 129
DOI: 10.11159/cdsr22.129

Leader-Follower Formation with Second-Order Slide Mode Control for Differential-Drive Mobile Robots

Mario Ramirez-Neria[1], Jaime González-Sierra[2], Eduardo G. Martinez-Hernandez[1]
Rodrigo Ramirez-Juarez[1] and Pablo Paniagua-Contro[1]
[1]InIAT Institute of Applied Research and Technology, Universidad Iberoamericana Ciudad de México.
Prolongación Paseo de la Reforma 880, Colonia Lomas de Santa Fe, CP 01219, México.
mario.ramirez@ibero.mx; eduardo.gamaliel@ibero.mx; juarezrgo@gmail.com; pablo.paniagua@ibero.mx
[2]Universidad Politécnica de Pachuca
Carretera Pachuca-Cd. Sahagún km 20 Ex-Hacienda de Santa Bárbara, 43830, Zempoala, Hidalgo, México.
jamesgsjr@hotmail.com

Abstract **–** In this paper, the leader-follower formation control of two differential-drive mobile robots is addressed using the inter-robot distance and the heading angle. To avoid singularities in the control law, a point located at a certain distance from the midpoint of the wheel axle, is considered as the output of the system. The proposed control strategy is designed using a second-order sliding mode and, therefore, is robust against bounded disturbances. It is worth noting that the decentralized control strategy only depends on local information about distance and the heading angle measurements. Real-time experiments show the performance of the approach.

Keywords**:** Differential-drive robots, Sliding mode control, Leader-follower.

1. Introduction

The coordination of multiple mobile robots has been studied widely by researchers and practitioners. The theoretical studies allowed the development of several mobile robots applications in the industry, vigilance, package delivery, home services, logistics, among others [1]. The multiple robot coordination extends the classical point convergence and trajectory tracking control strategies applied a unique mobile robot for the case of the collective behaviours like the convergence to formation patterns, formation tracking, dispersion, containment, inter-robot collision avoidance, etc [2].

The formation tracking requires the convergence of a set of robots to a formation pattern and a trajectory concurrently. The most basic scheme of formation tracking is the case of two robots. A leader robot follows a desired trajectory while the follower agent is controlled to achieve a desired relative posture and orientation with respect to the leader robot [3]. In a decentralized scheme, the control methodology depends on the local measurements of relative distance or angles [4]. In [5], the authors present the extension of leader-follower behaviours, for the case of a combined set of kinematic models of omnidirectional and differential-drive wheeled mobile robots. The approaches are based on the decentralized measurements of distance and heading angles. Nevertheless, if the leader and follower robots are the so-called differential-drive mobile robots, a restriction appears to define a linearizing feedback control law, when the angle between agents falls in $\pm\frac{\pi}{2}$.

On the other hand, the Slide Mode Control (SMC) methodology [6] is a robust control based on relay control, despite his chattering drawback. In order to avoid the chattering effects by the discontinuous nature of the SMC, a second-order SMC algorithm [7] is proposed to control the leader-follower scheme. This approach is a continuous controller with all the main properties of a first-order SMC such as eliminate disturbances or perturbations. Additionally, the connection between leader and follower has been developed by using Cartesian coordinates in [8].

This paper focuses on design a robust control strategy to solve the leader-follower formation control based on the local measurements between a pair of differential-drive mobile robots. Such control strategy is designed using a second-order SMC depending on the feedback of the distance and heading angle. Furthermore, the main contribution of this article is avoid the angle restriction appeared in the leader-follower differential-drive scheme. To do this, the output of the kinematic model defined as the control target is a point located at a distance from the midpoint of the wheel axle.

2. The leader-follower problem

Consider a set of two differential-drive mobile robots moving in a horizontal plane according to Fig. 1.

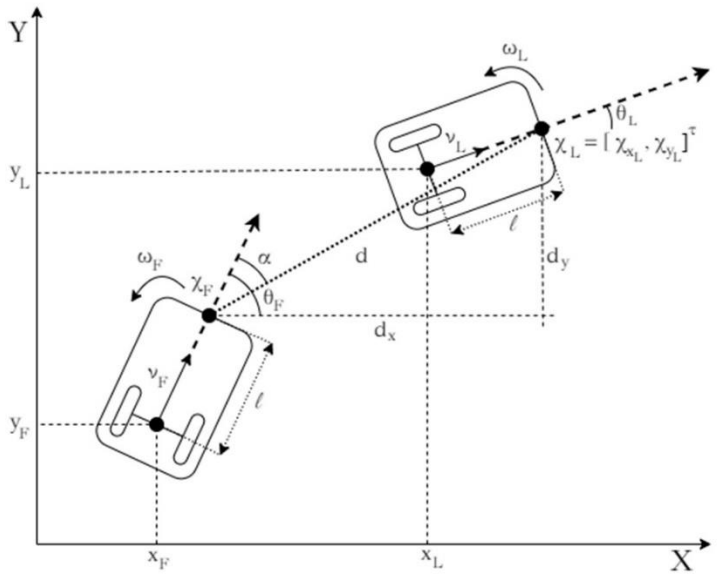

Fig. 1. Schematic diagram for two differential-drive mobile robots under the leader-follower approach.

The equations describing the kinematic motion of these differential-drive mobile robots are defined as

$$\dot{\boldsymbol{\xi}}_{\boldsymbol{i}} = \boldsymbol{G}(\theta_i)\boldsymbol{u}_{\boldsymbol{i}}, \tag{1}$$

for $i = L, F$, where the sub-index L corresponds to the leader agent and F is the follower. The system matrix $\mathbf{G}(\theta_i)$ is defined by

$$\boldsymbol{G}(\theta_i) = \begin{bmatrix} \cos\theta_i & 0 \\ \sin\theta_i & 0 \\ 0 & 1 \end{bmatrix}, \tag{2}$$

where $\boldsymbol{\xi}_{\boldsymbol{i}} = [x_i \quad y_i \quad \theta_i]^T$ is the state vector with $x_i, y_i \in \mathbb{R}$ as the position in the plane of the *i-th* agent, $\theta_i \in \mathbb{R}$ is the orientation angle respect to the horizontal axis and $\boldsymbol{u}_{\boldsymbol{i}} = [v_i \quad \omega_i]^T$ is the control input vector with $v_i \in \mathbb{R}$ the longitudinal velocity and $\omega_i \in \mathbb{R}$ the angular velocity.

2.1 Problem Statement

It is well known that when trying to control the coordinates x_i, y_i from (1), it cannot be stabilized with a continuous and time-invariant control law due to singularities in the controller [9]. Thus, it is proposed to study the kinematics of a point χ_i located at a distance l from the midpoint of the wheel axle, in order to avoid such singularities. This point is given by

$$\chi_i = \begin{bmatrix} \chi_{xi} \\ \chi_{yi} \end{bmatrix} = \begin{bmatrix} x_i + l\cos\theta_i \\ y_i + l\sin\theta_i \end{bmatrix}. \tag{3}$$

for $i = L, F$. The kinematics of point χ_i is given as

$$\dot{\chi}_i = \begin{bmatrix} \dot{\chi}_{xi} \\ \dot{\chi}_{yi} \end{bmatrix} = A_i(\theta_i, l)\boldsymbol{u_i}, \quad (4)$$

with

$$A(\theta_i, l) = \begin{bmatrix} \cos\theta_i & -l\sin\theta_i \\ \sin\theta_i & l\cos\theta_i \end{bmatrix}, \quad (5)$$

as the non-singular decoupling matrix since $\det\big(A(\theta_i, l)\big) = l$.

2.2 Leader-follower formation based on distance and heading angle

It is desired to obtain a dynamic model that describes the motion of the robots as a function depending on the distance d and the heading angle α [3],[5], i.e.

$$\dot{\eta} = [\dot{d} \quad \dot{\alpha}]^T = f(\theta_L, \quad \theta_F, \quad u_L, \ u_F, \quad \alpha, \quad d), \quad (6)$$

Note by Fig. 1, that $d \in \mathbb{R}$ is the Euclidian distance measured from the front point of the follower to the front point of the leader, with d_x and $d_y \in \mathbb{R}$ being the components of $\vec{d}$. Also, $\alpha \in \mathbb{R}$ is the heading angle measured from the distance vector $\vec{d}$. Therefore, the main goal is to design a control strategy such that the follower robot keeps a desired distance d^* and a desired heading angle α^* with respect to the leader robot.

Let us define $d_x = \chi_{xL} - \chi_{xF}$ and $d_y = \chi_{yL} - \chi_{yF}$ (see Fig. 1), then

$$d = |\vec{d}| = \sqrt{(\chi_{xL} - \chi_{xF})^2 + \left(\chi_{yL} - \chi_{yF}\right)^2} = \sqrt{d_x^2 + d_y^2}, \quad (7)$$

$$\alpha = \theta_F - \tan^{-1}\left(\frac{\chi_{yL} - \chi_{yF}}{\chi_{xL} - \chi_{xF}}\right) = \theta_F - \tan^{-1}\left(\frac{d_y}{d_x}\right). \quad (8)$$

The time-derivative of d, α, d_x and d_y are obtained using (4)-(5) and (7)-(8) as follows

$$\dot{d} = \frac{d_x\,\dot{d}_x + d_y\,\dot{d}_y}{d}, \quad (9)$$

$$\dot{\alpha} = \dot{\theta}_F - \frac{d_x\dot{d}_y - d_y\,\dot{d}_x}{d^2}, \quad (10)$$

$$\dot{d}_x = v_L\cos\theta_L - v_F\cos\theta_F + l\omega_F\sin\theta_F - l\omega_L\sin\theta_L, \quad (11)$$

$$\dot{d}_y = v_L\sin\theta_L - v_F\sin\theta_F - l\omega_F\cos\theta_F - l\omega_L\cos\theta_L. \quad (12)$$

Substituting (11)-(12) into (9)-(10) and considering $d_x = d\cos(\theta_F - \alpha)$ and $d_y = d\sin(\theta_F - \alpha)$, the kinematics of d and α is expressed as follows

$$\begin{bmatrix} \dot{d} \\ \dot{\alpha} \end{bmatrix} = \begin{bmatrix} \cos(\alpha - \theta_F + \theta_L) & -l\sin(\alpha - \theta_F + \theta_L) \\ -\frac{l}{d}\sin(\alpha - \theta_F + \theta_L) & -\frac{l}{d}\cos(\alpha - \theta_F + \theta_L) \end{bmatrix}\begin{bmatrix} v_L \\ \omega_L \end{bmatrix} - \begin{bmatrix} \cos(\alpha) & -l\sin(\alpha) \\ -\frac{1}{d}\sin(\alpha) & -1 - \frac{l}{d}\cos(\alpha) \end{bmatrix}\begin{bmatrix} v_F \\ \omega_F \end{bmatrix}. \quad (13)$$

In matrix form, the following system is obtained

$$\dot{\eta} = A(\theta_F, \quad \theta_L, \quad \alpha, \ d\ )u_L - B(\alpha, \quad d)u_F, \quad (14)$$

with $\eta = [d \quad \alpha]^T$ as the state vector and matrices A and B defined as

$$A = \begin{bmatrix} \cos(\alpha - \theta_F + \theta_L) & -l\sin(\alpha - \theta_F + \theta_L) \\ -\frac{l}{d}\sin(\alpha - \theta_F + \theta_L) & -\frac{l}{d}\cos(\alpha - \theta_F + \theta_L) \end{bmatrix}, \qquad B = \begin{bmatrix} \cos(\alpha) & -l\sin(\alpha) \\ -\frac{1}{d}\sin(\alpha) & -1 - \frac{l}{d}\cos(\alpha) \end{bmatrix}.$$

Note that the matrix B is no singular since $\det(B) = -\left(\frac{l}{d} + \cos\alpha\right)$. If $d \neq l$ and $\cos\alpha \neq \pm(2n+1)\pi$ for $n = 0,1,\cdots\infty$, then any angle α can be chosen between robots for $d \gg l$. It will prevent robots from colliding with each other.

Let us define the desired vector $\eta^* = [d^* \quad \alpha^*]^T$. Therefore, it is possible to define the tracking error as $e_\eta = \eta - \eta^*$. The dynamics of the tracking error is obtained as follows

$$\dot{e}_\eta = \dot{\eta} - \dot{\eta^*}, \tag{15}$$

$$\dot{e}_\eta = A(\theta_F, \quad \theta_L, \quad \alpha, \ d\ )u_L - B(\alpha, \quad d)u_F - \dot{\eta^*}. \tag{16}$$

Note that (16) can be simplified to a perturbed dynamic error system as

$$\dot{e}_\eta = -B(\alpha, \quad d)u_F + \phi_F(t), \tag{17}$$

where $\phi_F(t)$ is the perturbation vector of the follower robot that must be estimated or cancelled, given by

$$\phi_F(t) = A(\theta_F, \quad \theta_L, \quad \alpha, \ d\ )u_L - \dot{\eta^*}. \tag{18}$$

3. Control design

In this section, a second-order SMC is designed so that the leader follows a desired trajectory while the follower maintains a distance and heading angle from the leader.

3.1 Second-order SMC for the follower robot

Consider the perturbed dynamic error of the follower robot given in (17) and the following slide mode surface using the tracking error

$$\sigma_F = e_\eta + \beta_F \int e_\eta \, dt, \tag{19}$$

where β_F is a 2×2 matrix gain. Taking the time-derivative of (19), it is obtained

$$\dot{\sigma_F} = \dot{e}_\eta + \beta_F e_\eta. \tag{20}$$

Then, substituting the error dynamics (17), it gives

$$\dot{\sigma_F} = -B(\alpha, \quad d)u_F + \Psi_F(t), \tag{21}$$

where the *total disturbance* is defined as follows

$$\Psi_F(t) = \phi_F(t) + \beta_F e_\eta. \tag{22}$$

Therefore, a second-order SMC is proposed for the follower agent as

$$u_F = B(\alpha, \quad d)^{-1}(\Lambda_F \sigma_F + v), \tag{23}$$

$$\dot{v} = M_F sign(\sigma_F), \tag{24}$$

with the control gains defined as

$$\beta_F = \begin{bmatrix} \beta_{1F} & 0 \\ 0 & \beta_{2F} \end{bmatrix}, \quad \Lambda_F = \begin{bmatrix} \lambda_{1F} & 0 \\ 0 & \lambda_{2F} \end{bmatrix}, \quad \text{and} \quad \mathrm{M}_F = \begin{bmatrix} m_{1F} & 0 \\ 0 & m_{2F} \end{bmatrix}. \tag{25}$$

with $\beta_{1F}, \beta_{2F}, \lambda_{1F}. \lambda_{2F}, m_{1F}$ and m_{2F} are positive constants.

3.2 Second-order SMC for the leader robot

Consider the kinematics of the leader robot given in the equation (4)

$$\dot{\chi_L} = A_L(\theta_L, l)u_L. \tag{26}$$

Let us define the leader tracking error $e_L = \chi_L - \chi^*$ with $\chi^* = \begin{bmatrix} {\chi_x}^* & {\chi_y}^* \end{bmatrix}^T$ as the desired trajectory. Taking the time-derivative of the leader tracking error, it is obtained

$$\dot{e}_L = A_L(\theta_L, l)u_L - \chi^*. \tag{23}$$

Using (23), the following slide mode surface is proposed

$$\sigma_L = e_L + \beta_L \int e_L \, dt, \tag{24}$$

where β_L is a 2×2 matrix gain. Taking the time-derivative of (28), it gives

$$\dot{\sigma_L} = \dot{e}_L + \beta_L e_L, \tag{29}$$

then, substituting the error dynamics (23) into (29)

$$\dot{\sigma_L} = A_L(\theta_L, l)u_L + \Psi_L(t), \tag{30}$$

where the *total disturbance* of the leader robot is defined as follows

$$\Psi_L(t) = \beta_L e_L - \chi^*. \tag{31}$$

Thus, a second-order SMC is proposed for the leader robot as

$$u_L = -A_L(\theta_L, l)^{-1}(\Lambda_L \sigma_L + v_L), \tag{32}$$

$$\dot{v_L} = M_L sign(\sigma_L), \tag{33}$$

with the controller gains defined as

$$\beta_L = \begin{bmatrix} \beta_{1L} & 0 \\ 0 & \beta_{2L} \end{bmatrix}, \quad \Lambda_L = \begin{bmatrix} \lambda_{1L} & 0 \\ 0 & \lambda_{2L} \end{bmatrix}, \quad \text{and} \quad \mathrm{M}_L = \begin{bmatrix} m_{1L} & 0 \\ 0 & m_{2L} \end{bmatrix}. \tag{34}$$

where $\beta_{1L}, \beta_{2L}, \lambda_{1L}. \lambda_{2L}, m_{1L}$ and m_{2L} are positive constants.

4. Experimental Implementation

The experimental platform is described in the first part of this Section. After that, a real-time experiment is presented showing the performance of the proposed control strategy.

4.1 Experimental setup for the leader and follower robots

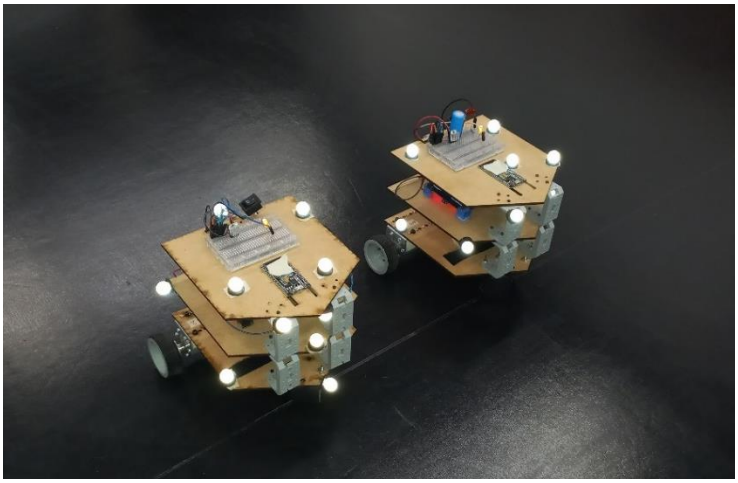

Fig. 2 Leader and follower differential-drive mobile robots.

Fig. 2 shows the prototypes of the differential-drive mobile robots used in the experimental work. Each robot was using two 12V POLOLU 37D gear motors, with gear ratio 1: 19 and a built-in encoder with 64 counts per revolution. STM32F4 Discovery board is used as a data acquisition device. The communication between the computer and the done in real-time using the publicly available "waijung1504a" Matlab/Simulink library via Bluetooth using a ESP32 microcontroller. The wheel radius is given by $r = 0.03$[m] and the distance $l = 0.11$[m] from the mid-point of the wheels' axle to the frontal point. Furthermore, two PI controllers with anti-windup are implemented to control the velocity of each motor using $0.005s$ sampling time. The gains of the on-board PI controllers were established for each motor to: $kp = 6, k_i = 60$, and $T_t = 0.1$. The position and orientation of the differential-drive mobile robots are measured using a set of 10 infrared VICON cameras with resolution of 0.0005[m] and a workspace of $6x6$[m^2] with a sampling time of 0.005[s].

4.2 Experimental results

The trajectory in the plane of both mobile robots is depicted in Fig. 3. The leader robot is controlled to follow a circular trajectory of 0.5[m] of radius while the follower robot keeps a desired distance $d^* = 0.3$[m] and a desired heading angle $\alpha^* = \frac{\pi}{2}$ radians. The gains for the follower robot were selected as $\beta_{1F} = 2$, $\beta_{2F} = 3$, $\lambda_{1F} = 2$, $\lambda_{2F} = 3$, $m_{1F} = 0.01$, $m_{2F} = 0.01$ and for the leader robot as $\beta_{1L} = 4$, $\beta_{2L} = 3$, $\lambda_{1L} = 4$, $\lambda_{2L} = 3$, $m_{1L} = 0.01$ and $m_{2L} = 0.01$.

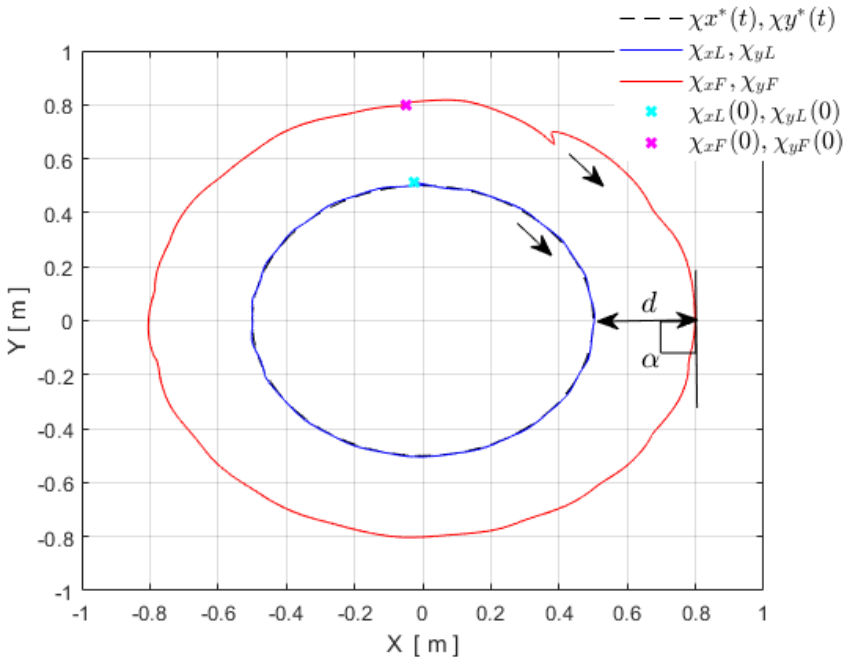

Fig. 3. Trajectories of the leader and follower robots.

The position error of the leader robot is illustrated in Fig. 4. It becomes evident that these errors oscillate around zero. This is due to the fact that there are noise measurements, non-modeled dynamics, among others. The Fig. 5 presents the control inputs required for the leader robot to perform his motion and reach the desired trajectory. On the other hand, the distance and heading angle between robots is shown in Fig. 6. Note that the distance and heading angle converge to their desired values. Finally, Fig. 7 presents the control inputs for the follower robot.

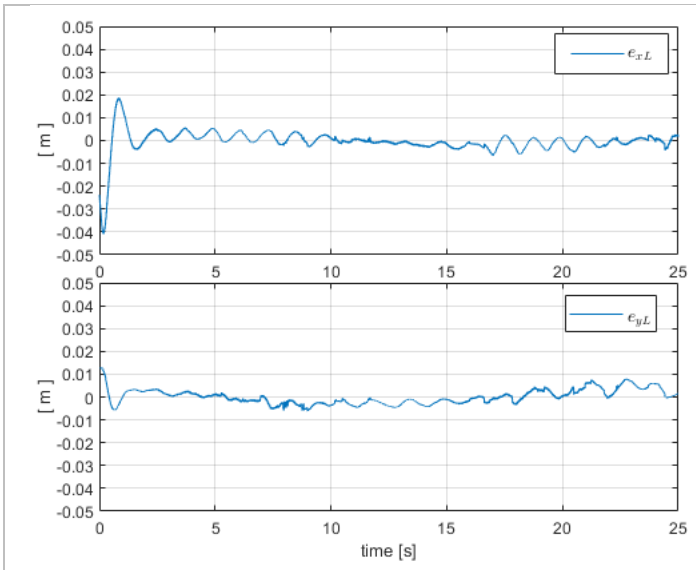

Fig. 4. Position error for the leader.

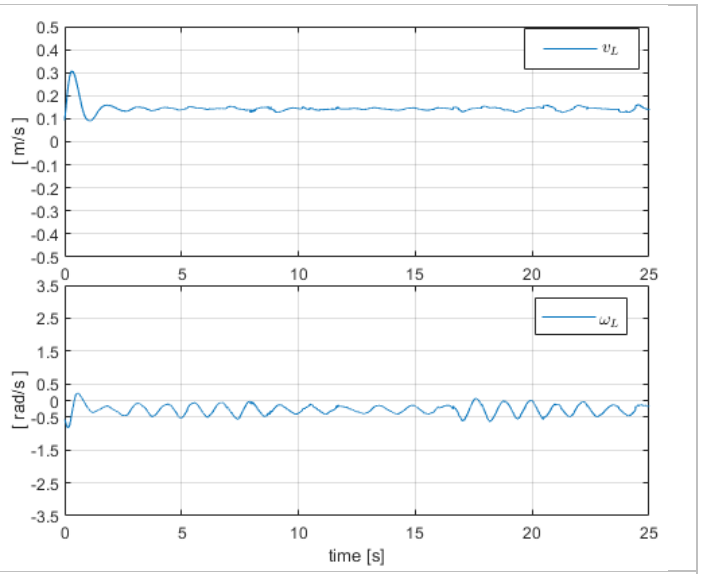

Fig. 5. Control inputs for the leader.

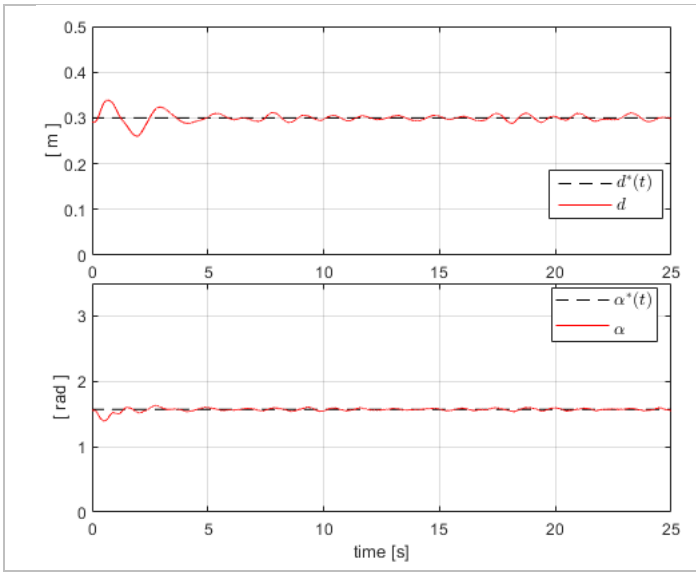

Fig. 6. Distance and formation angle between the follower and the leader.

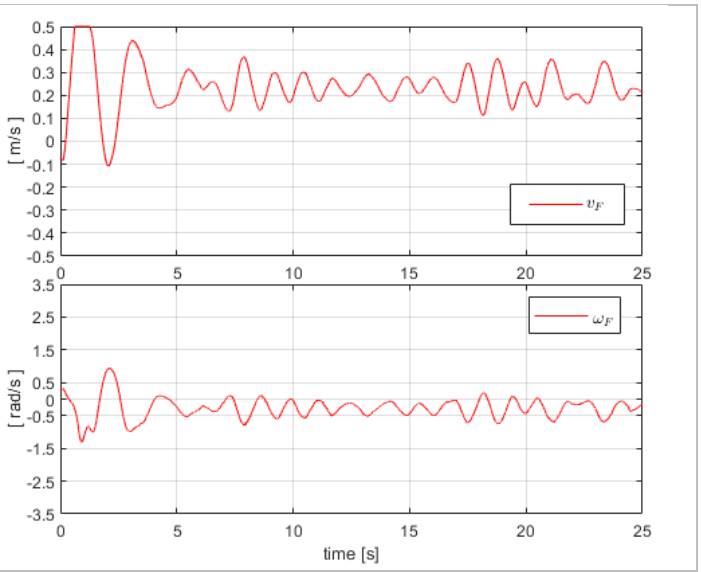

Fig. 7. Control inputs for the follower.

5. Conclusion

In this work is proposed a robust control strategy based on a second-order SMC to achieve a formation control between a leader and follower robot with differential-drive kinematical model. The leader robot converges to a desired trajectory while the follower agent converges to a desired distance and heading angle with respect to the leader. The formation control law is designed to be dependent only on the local measurement of the distance and heading angle. Therefore, the approach becomes a decentralized alternative to be implemented using a local sensor on board the robots.

The performance of the proposed control law is validated by real-time experiments. In further research, the leader-follower approach will be extended to other non-holonomic mobile robots and other formation graphs.

Acknowledgements

This work was supported by the Universidad Iberoamericana Ciudad de México, through the Project Grant DINVP-0025.

References

[1] W. Ren and R. Beard, "Distributed Consensus in Multi-vehicle Cooperative Control", Springer, London, UK, 2008.

[2] J. P. Desai, J. P. Ostrowski, and V. Kumar, "Modeling and control of formations of nonholonomic mobile robots," *IEEE Transactions on Robotics and Automation*, 2001, vol. 17, no. 6, pp. 905– 908,

[3] J. González-Sierra, E. G. Hernandez-Martinez, E. Ferreira-Vazquez, J. Flores-Godoy, G. Fernandez-Anaya and P. Paniagua-Contro, "Leader-follower Control Strategy with Rigid Body Behavior", in *Proceedings of the Symposium of Robot Control*, Budapest, Hungary, 2018, vol. 51-22, pp. 184-189.

[4] E. G. Hernandez-Martinez and E. Aranda-Bricaire, "Trajectory tracking for groups of unicycles with convergence of the orientation angles", *in Proceedings of the 49th IEEE Conference on Decision and Control (CDC),* Atlanta, GA, USA, 2010, pp. 6323-6328.

[5] P. Paniagua-Contro, E. G. Hernandez-Martinez, O. González-Medina, J. González-Sierra, J. Flores-Godoy, E. Ferreira Vazquez and G. Fernandez-Anaya, "Extension of Leader-Follower Behaviours for Wheeled Mobile Robots in Multirobot Coordination", *Mathematical Problems in Engineering*, vol. 2019, pp. 1-16, 2019.

[6] J. Rivera, L. Garcia, C. Mora, J. Raygoza, and S. Ortega. "Super-twisting sliding mode in motion control systems". *Sliding mode control 1*, 2011, pp. 237-254.

[7] A. Chalanga, S. Kamal, L. M. Fridman, B. Bandyopadhyay, and , J. A. Moreno, "Implementation of super-twisting control: Super-twisting and higher order sliding-mode observer-based approaches". *IEEE Transactions on Industrial Electronics*, 2016, vol. 63, no. 6, pp. 3677-3685.

[8] E. G. Hernandez-Martinez and E. Aranda-Bricaire, "Decentralized formation control of multi-agent robot systems based on formation graphs", *Studies in Informatics and Control*, 2012, vol. 21, pp. 7-16.

[9] R. W. Brockett, "Asymptotic Stability and Feedback Stabilization", *In: R. W. Brockett, R. S. Millman and H. J. Sussman editors, Differential Geometric Control Theory, Birkhauser*, 1983, pp. 181-191.